

A new ankylosaurid (Dinosauria: Ankylosauria) from the Lower Cretaceous of China, with comments on ankylosaurian relationships

Matthew K. Vickaryous, Anthony P. Russell, Philip J. Currie, and Xi-Jin Zhao

Abstract: Amongst the fossil material collected by the Sino-Soviet Expeditions (1959–1960) to the Alshan Desert, China, was a large, virtually complete ankylosaur skeleton. *Gobisaurus domoculus* gen. et sp. nov. closely resembles *Shamosaurus scutatus*, but is distinct in having an unfused basipterygoid–pterygoid contact and elongate premaxillary processes of the vomers. Although it is difficult to make a definitive taxonomic assignment without considering postcranial material, a preliminary phylogenetic analysis places *Gobisaurus* as the sister taxon of *Shamosaurus*, clustered as one of several successive outgroups of the Ankylosaurinae.

Résumé : Parmi le matériel fossilifère recueilli lors des expéditions sino-soviétiques (1959–1960) dans le désert d’Alshan, en Chine, se retrouvait un gros ankylosaure presque complet. *Gobisaurus domoculus*, n. gen. et n. sp. ressemble de près à *Shamosaurus scutatus*, mais il s’en distingue par le contact basiptérygoïde–ptérygoïde non soudé et des processus prémaxillaires des vomers allongés. Bien qu’il soit difficile de procéder à une affectation taxonomique définitive sans considérer le matériel postcranien, une analyse phylogénétique préliminaire définit *Gobisaurus* comme un taxon ayant un lien parental avec *Shamosaurus*, regroupé en tant qu’un de plusieurs exogroupes successifs d’Ankylosaurinae.

[Traduit par la Rédaction]

Introduction

In 1959–1960, fieldwork was conducted in Inner Mongolia, People’s Republic of China, jointly by the Institute of Vertebrate Paleontology and Paleoanthropology (IVPP), Beijing, China, and the Paleontological Institute, Moscow, U.S.S.R. The Sino-Soviet Expeditions were intended to follow up on the success of the Central Asiatic Expeditions of the American Museum of Natural History, New York, U.S.A. in 1922–1930. Amongst the abundant material collected from a locality north of Chilantai, in the Maortu region of the Alshan Desert (Fig. 1), was the large theropod *Chilantaisaurus maortuensis*, various (as yet undescribed) fossil plants, invertebrates, turtles, ornithopods, sauropods and a virtually complete ankylosaur skeleton (Hu 1964). The latter (IVPP V12563), believed to have been collected from the same locality as *Chilantaisaurus* (although no official documentation exists) closely resembles the Lower Cretaceous ankylosaurid *Shamosaurus scutatus* (Tumanova 1983). Largely forgotten for decades, the specimen resurfaced with the initiation of the Sino-Canadian Dinosaur Project, a joint venture between the IVPP, the Royal Tyrrell Museum of

Palaeontology, Drumheller, Alberta, and the Canadian Museum of Nature, Ottawa, Ontario, Canada. It was included in a major traveling exhibit (alternatively known as the “Dinosaur Project,” the “Greatest Show Unearthed,” and the “Dinosaur World Tour”; Currie 1997), from 1990–1997, during which time it was referred to as “*Gobisaurus*.” This informal appellation was apparently an attempt to separate it from, yet ally it with, the genus *Shamosaurus* (*shamo* is an old Mongolian term for Gobi). Detailed examination of this specimen indicates that *Gobisaurus* represents a new taxon of Late Cretaceous ankylosaurid. The present contribution considers only the holotype cranium of *Gobisaurus*, as the postcranium was unavailable for study.

Institutional abbreviations

AMNH, American Museum of Natural History, New York, N.Y., U.S.A.; BM(NH), British Museum (Natural History), London, U.K.; CEUM, College of Eastern Utah, Price, Utah, U.S.A.; DMNH, Denver Museum of Natural History, Denver, Colorado, U.S.A.; GI, Geological Institute, Section of Paleontology, Ulaanbaatar, Mongolia; IVPP, Institute of Vertebrate Paleontology and Paleoanthropology, Beijing,

Received February 2, 2001. Accepted June 18, 2001. Published on the NRC Research Press Web site at <http://cjcs.nrc.ca> on November 21, 2001.

Paper handled by Associate Editor H.-D. Sues.

M.K. Vickaryous¹ and **A.P. Russell**. Vertebrate Morphology and Palaeontology Research Group, Department of Biological Sciences, University of Calgary, 2500 University Dr. N.W., Calgary, AB T2N 1N4, Canada.

P.J. Currie. Royal Tyrrell Museum of Palaeontology, P.O. Box 7500, Drumheller, AB T0J 0Y0, Canada.

X.-J. Zhao. Institute of Vertebrate Paleontology and Paleoanthropology, Academia Sinica, P.O. Box 643, Beijing 100044, People’s Republic of China.

¹Corresponding author: Present address: Department of Biology, Dalhousie University, Life Sciences Centre, Halifax, NS B3H 4J1, Canada (e-mail: mickary@is2.dal.ca).

Fig. 1. Schematic map of China and Mongolia illustrating the approximate locality of *Gobisaurus domoculus* (closed star symbol) and the reported localities of *Shamosaurus scutatus* (open star symbols). Circles denote urban centres (capital cities underlined). Scale bar represents 1000 km.



People's Republic of China; NMC, Canadian Museum of Nature, Paleobiology Division (National Museum of Canada), Ottawa, Ontario, Canada; SMU, Shuler Museum of Paleontology, Dallas, Texas, U.S.A.; TMP, Royal Tyrrell Museum of Palaeontology, Drumheller, Alberta, Canada; UALVP, University of Alberta Laboratory of Vertebrate Palaeontology, Department of Geology, Edmonton, Alberta, Canada; USNM, National Museum of Natural History (formerly the United States National Museum), Washington, D.C., U.S.A.

Systematic palaeontology

Dinosauria Owen 1842
 Ornithischia Seeley 1888
 Ankylosauria Osborn 1923
 Ankylosauridae Brown 1908

Gobisaurus gen. nov.

Type species

Gobisaurus domoculus.

Etymology

Gobi, refers to the geographic locale.

Diagnosis

Large ankylosaurid with orbits 20% of cranial length and external nares 23% of cranial length; robust basipterygoid processes not fused to main pterygoid body; elongate premaxillary processes of vomers visible in palatal view.

Similar to *Shamosaurus* in having delta-shaped dorsal profile, with premaxillae forming narrow apex. Differs from *Shamosaurus* in that cranium longer than wide; lacks discernible cranial sculpturing over antorbital area; maxillary tooth row length compared to overall cranium length relatively shorter;

maximum premaxillary rostrum width greater than distance between the posteriormost maxillary teeth; reduced supraorbital bosses; and anterior surface of pterygoid vertically oriented.

Gobisaurus domoculus sp. nov.

Holotype

IVPP V12563

Type locality

IVPP V12563 is believed to have been collected from the same general locality as the large theropod *Chilantaisaurus maortuensis*, approximately 60 km north of Chilantai (Jilantai; 39 45 N, 105 45E), on the east side of Chilantai Salt Lake (Chilantaiyen Chih), Maortu, Alashan Desert, Nei Mongol Zizhique (Inner Mongolia), China.

Formation

Ulanhushao (Suhongtu) Formation, Lower Cretaceous (Aptian–?Albian).

Etymology

domo to subjugate; and oculus, the eye.

Diagnosis

As for the genus, as it is the only known species.

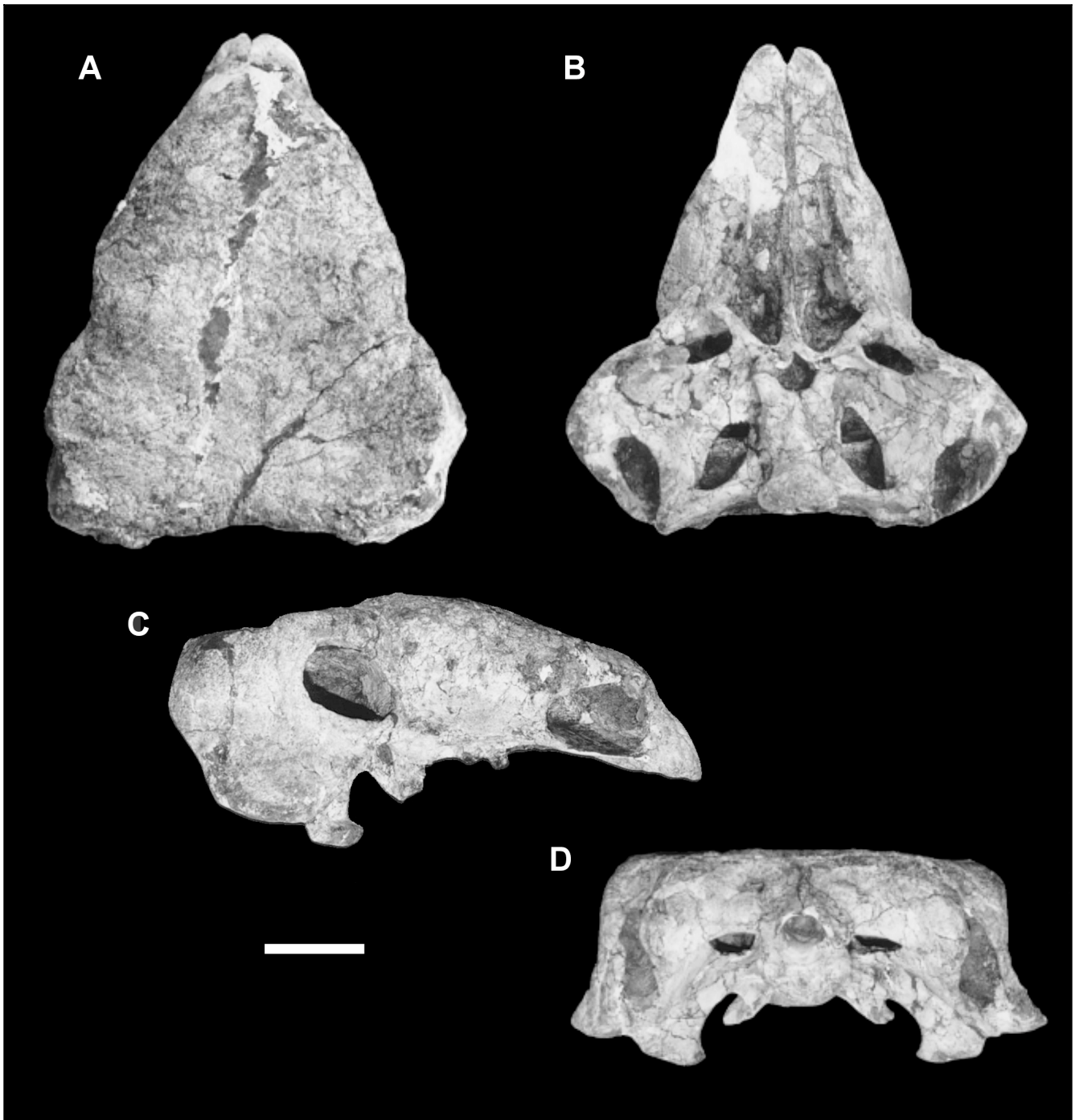
Description

The cranium is well-ossified and virtually complete (Figs. 2A–2D), measuring 457 mm from the anterior (rostral; Baumel et al. 1993) tips of the premaxillary to the posterior (caudal; Baumel et al. 1993) edge of the occipital condyle. In dorsal view (Fig. 2A), the cranium is triangular and slightly longer than wide (445 mm between the flaring, rounded apices of the quadratojugal bosses). The entire dorsum is covered with a rugose, pockmarked texture that lacks any organized pattern of ornamentation (Coombs 1971; Vickaryous et al. 2001). Except for a short segment of the sagittal interpremaxillary suture, none of the cranial sutures are visible in dorsal (Fig. 2A) or lateral view (Figs. 2C, 3).

Neither the dorsotemporal nor the antorbital fenestrae are visible. In addition, the laterotemporal fenestrae are obscured from lateral view by the squamosal–quadratojugal complex. The remaining openings, the anterolaterally directed external nares and orbits, are prominent (Figs. 2C, 3). The roughly elliptical nasal vestibula occupy over 23% of the cranial length (long-axis is 106.6 mm), and are subdivided medially by posterodorsally oriented narial septa, derived from a process from each premaxilla. Computer tomography (CT) scans (Fig. 3) suggest that the anterior narial opening (the nasal aperture) leads to the nasal cavity proper, while the posterior narial opening (the paranasal aperture) leads to a paranasal sinus cavity.

The orbit of *Gobisaurus* is ovoid, with the long-axis oriented, such that the narrowest end is directed anteroventrally (Figs. 2C, 3). Its long-axis (91.5 mm) accounts for 20% of the cranial length. A narrow rim of bone encircles the orbit, gaining prominence along the anterior and ventral borders, before becoming confluent with the supraorbital boss. The orbital cavity is bounded by the basicranium medially, the

Fig. 2. Cranium of *Gobisaurus domoculus* gen. et sp. nov. in dorsal (A), ventral (B), right lateral (C), and occipital (D) views. IVPP V12563, holotype. Scale bar represents 100 mm.



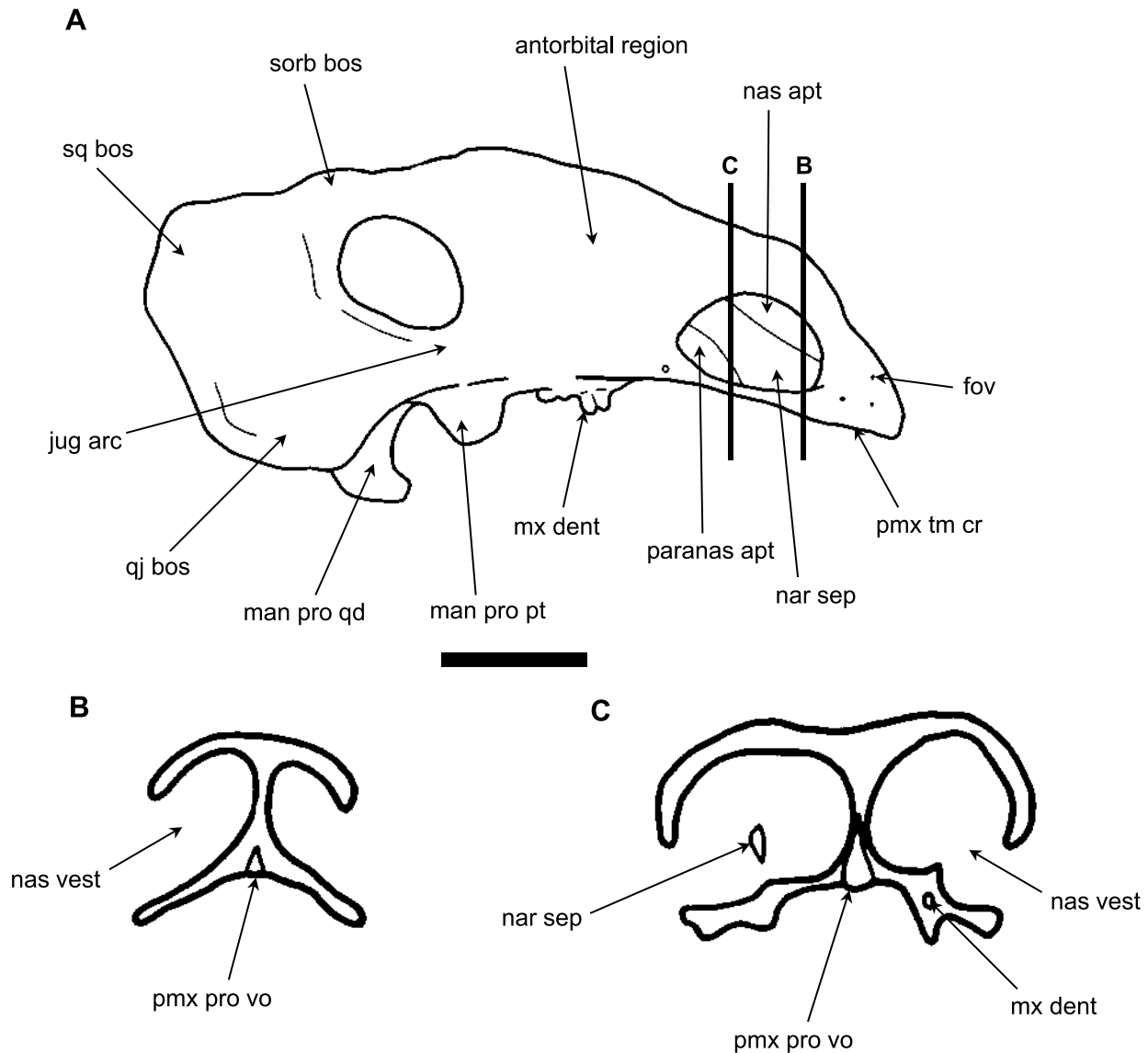
postocular shelf posteriorly, and the skull table dorsally. A bony wall marks the anterior margin of the orbital cavity, although the identification of the elements composing this structure remains unclear. Concomitant with the enormous size of the orbits, the jugal arch is shallow.

The antorbital area is swollen (Figs. 2C, 3), extending from the posterior edge of the external naris to a position just anterodorsal to the orbit. A morphological reciprocity exists between the elliptical nasal vestibule, the ovoid orbit,

and the bulbous antorbital region, with the antorbital region situated as a trapezoid-like wedge between the prominent openings.

The maximum distance between the supraorbital bosses (Fig. 2A; 350 mm) is nearly equivalent to the maximum distance across the squamosal bosses (352 mm). Both the supraorbital and the squamosal bosses are rounded, blunt, and have low surface relief. In lateral view, the supraorbital boss appears continuous with the circumorbital rim.

Fig. 3. Lateral view of the cranium (A) and transverse sections (B and C) through the rostrum of *Gobisaurus domoculus*, interpretive illustration. IVPP V12563, holotype. Scale bar represents 100 mm. fov, fovea; jug arc, jugal arch; man pro pt, mandibular process of the pterygoid; man pro qd, mandibular process of the quadrate; mx dent, maxillary dentition; nar sep, narial septum; nas apt, nasal aperture; nas vest, nasal vestibule; paranas apt, paranasal aperture; pmx pro vo, premaxillary processes of the vomers; pmx tm cr, premaxillary tomial crest; qj bos, quadratojugal boss; sorb bos, supraorbital boss; sq bos, squamosal boss.

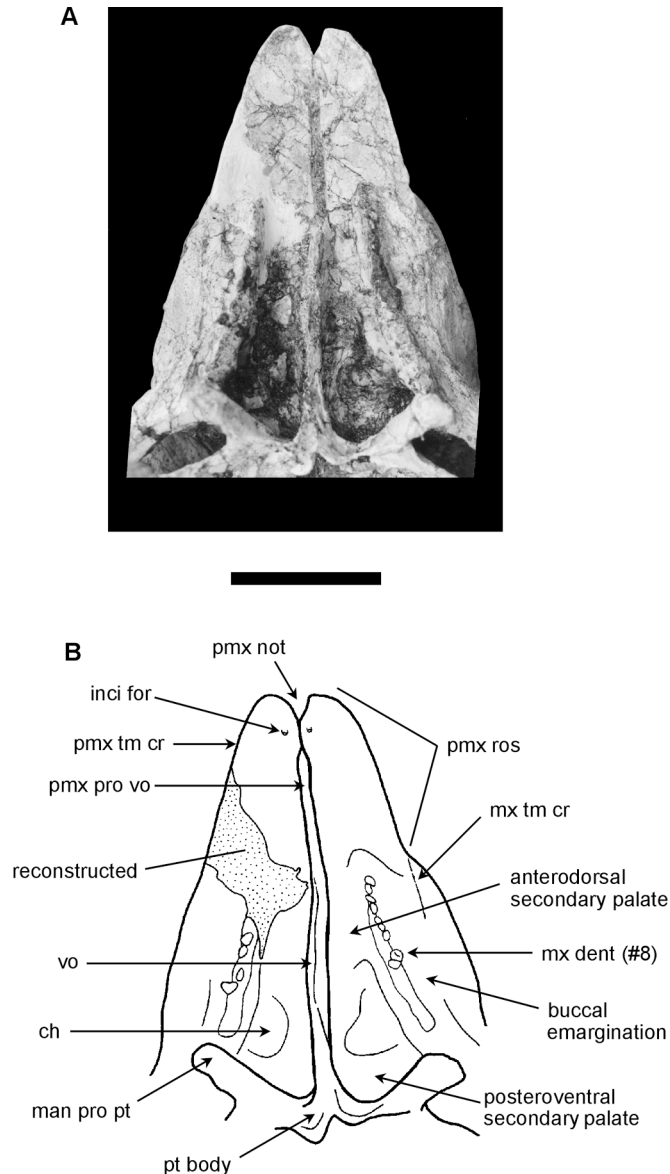


The premaxilla (Figs. 2, 3, 4) is edentulous, encloses the anterior half of the external naris, and bears a number of foveae and shallow vertically oriented furrows externally. Cranial ornamentation obscures the dorsal and lateral sutural contacts of the premaxilla with the adjacent dermatocranial elements and, with the exception of the short interpremaxillary articulation, only the sutures along the palate can be discerned. Along the narrow premaxillary palate, the interpremaxillary suture is deeply incised by a premaxillary notch (interpremaxillary notch; Sereno 1999; Fig. 4). The premaxillary tomial crests continue posteriorly from the notch and terminate posterior to the premaxillary–maxillary contact. In cross-section, the ventral surface of the premaxillary palate is a shallow concavity (Figs. 3A, 3B). Directly posterior to the premaxillary notch, along the palatal

surface of each premaxilla, is a posterodorsally inclined parasagittal incisive foramen (6 mm in diameter). Contact between the premaxillae along the palate is restricted to a narrow bridge medial to the incisive foramina. Posterior to this bridge, the premaxillae are separated by elongate anterior extensions of the vomers. The premaxilla–maxilla contact along the palate undulates anteriorly from the midpoint of the nasal vestibule, circumventing the alveolar border of the maxilla, then continuing posteromedially.

The topographic border of the maxilla is indistinguishable from the rest of the dermatocranium, except at the premaxillary contact along the palate (Figs. 2B, 4). The teeth are inset medially from the lateral border of the maxilla, forming a relatively flat buccal emargination (cheek pouch; Lee 1996). The tooth rows are maximally separated posteriorly (127

Fig. 4. Ventral view of the palate of *Gobisaurus domoculus*, original (A) and interpretive illustration (B). IVPP V12563, holotype. Scale bar represents 100 mm. ch, choana; inci for, incisive foramen; mx tm cr, maxillary tomial crest; pmx not, premaxillary notch; pmx ros, premaxillary rostrum; pt body, main body of the pterygoid; vo, vomer. Other abbreviations as in Fig. 3.



mm) and converge towards the rostrum (distance between tooth rows at the anteriormost tooth position is 95 mm). Proximal to the premaxillae, the tooth rows are parallel. Tooth row length is approximately 26.7% (122 mm) of cranial length. Although most of the alveolar bone is damaged and therefore an accurate tooth count is not possible, there are nine teeth preserved in situ in the left maxilla, and four in the right. Medially, the maxilla contributes to a large palatal shelf, the purported anterodorsal secondary palate (Coombs and Maryanska 1990) or anterior maxillary shelf (Tumanova 1983), forming the floor of the respiratory passage and the anterior rim of the choana. Bilaterally, each half of the anterodorsal secondary palate is inclined

posteromedially, contacting the vomers, pterygoids, and palatines. The sutural boundaries between these elements are not preserved.

Individual teeth are characterized by their relatively large size (cusp width up to 9.5 mm, maximum cusp height 11 mm) and the presence of a swollen base and an incipient cingulum along the lingual surface. The apical series of denticles is asymmetrically disposed across the medial–distal length of the tooth, but an exact count is not possible.

The vomers of *Gobisaurus* (Figs. 2B, 4) fuse into a thin keel, which while variably damaged along its palatal edge, extends ventrally beyond the plane of the palate to contact the premaxillae. Anteriorly, processes of the vomers intrude deeply into the premaxillary portion of the rostrum and unite with the roof of the premaxillary palate. CT scans (Figs. 3B, 3C) indicate that the united premaxillary processes of the vomers are triangular in cross-section and form a wedge between the premaxillae. Sutural contacts between the individual vomer elements, and between the vomers and the pterygoids, palatines, and maxillae, are not visible.

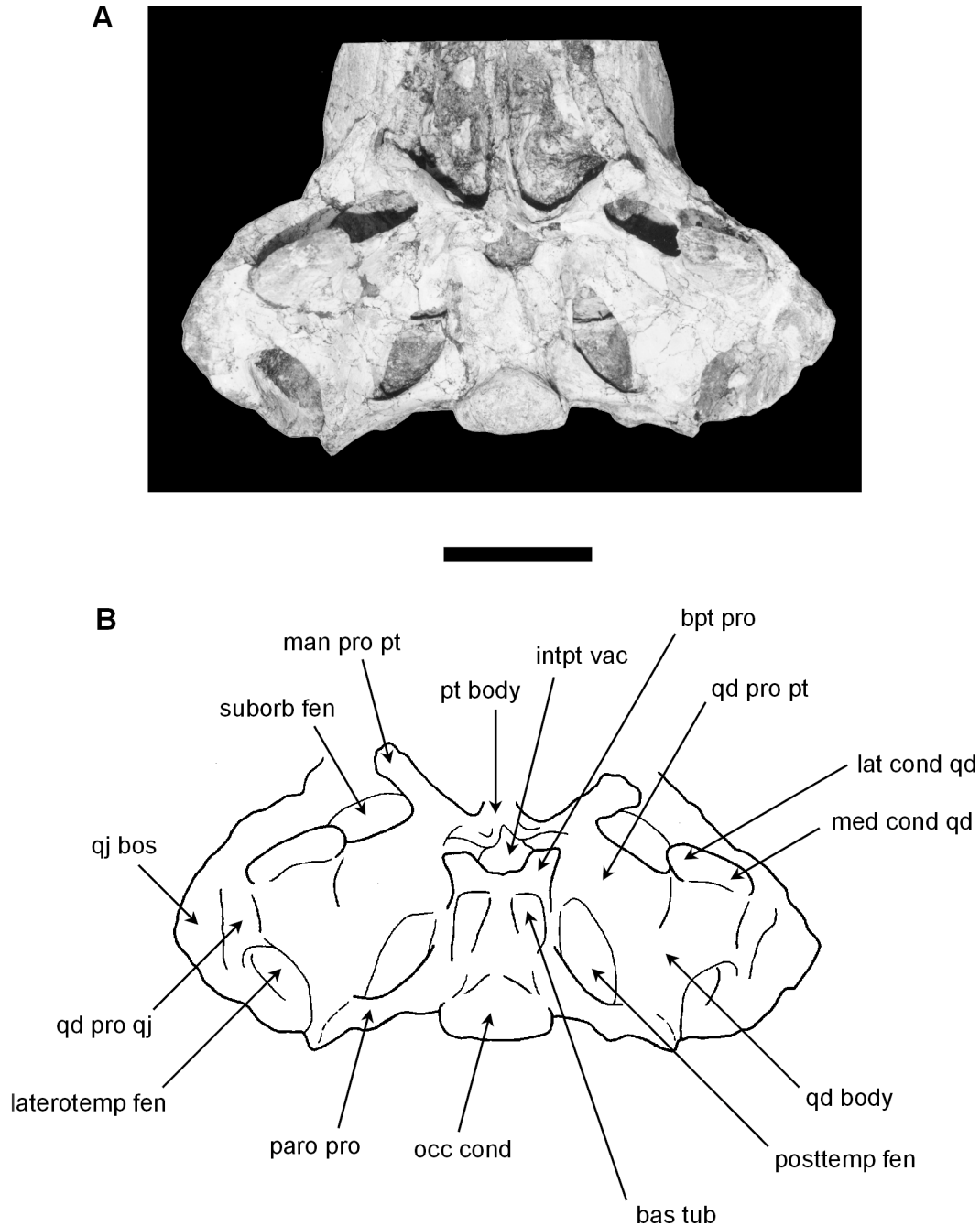
The main body of the pterygoid is vertically oriented, and abuts the vomer and the posteroventral secondary palate, the maxilla, the quadrate, and the basicranium (Figs. 2B, 4). Contacts between the pterygoid and the vomer and palatal shelf are obliterated. The pterygoid forms the anteromedial border of the suborbital fenestra. The anterolaterally directed mandibular process of the pterygoid fuses with the ectopterygoid near the posterior terminus of the maxillary tooth row. Distally, the mandibular process is expansive, slightly rugose, and directed laterally. The laminar quadrate process of the pterygoid is directed posterolaterally toward the quadrate. The suture between the pterygoid and the quadrate is not visible. The narrow gap between the main body of the pterygoid and each basiptyergoid process is bridged by matrix.

The ectopterygoid is short, deep, and directed anterolaterally. No sutures are visible between the ectopterygoid and the maxilla, palatine, or pterygoid.

Extensive fracturing of the palatines disallows full preparation, and contact between the palatine and the adjacent elements (e.g., maxilla, ectopterygoid, pterygoid) is difficult to discern, as none of the sutures are visible. Ventromedially, the palatine contributes to the posteroventral secondary palate (Figs. 2B, 4), along with the vomer, and defines the posterior limits of the choana.

The anteroventrally oriented quadrate (Figs. 2B, 2D, 5, 6) is fused with the quadratojugal laterally, the paroccipital process of the exoccipital dorsally, and the quadrate ramus of the pterygoid medially. The sutures between these elements are not readily distinguishable, although their positions may be deduced. Fusion between the quadrate and the pterygoid has eliminated the sutures in this region. The paroccipital process overlaps the squamosal process of the quadrate for nearly one-fourth of its vertical length. The squamosal process of the quadrate does not appear to fuse with the squamosal. The bicondylar mandibular process of the quadrate is located ventral to the posterior border of the orbit and projects ventrally well beyond the quadratojugal. The latter element is relatively broad, with a rounded apex that flares laterally. Contact with the quadrate was opposite to the apex.

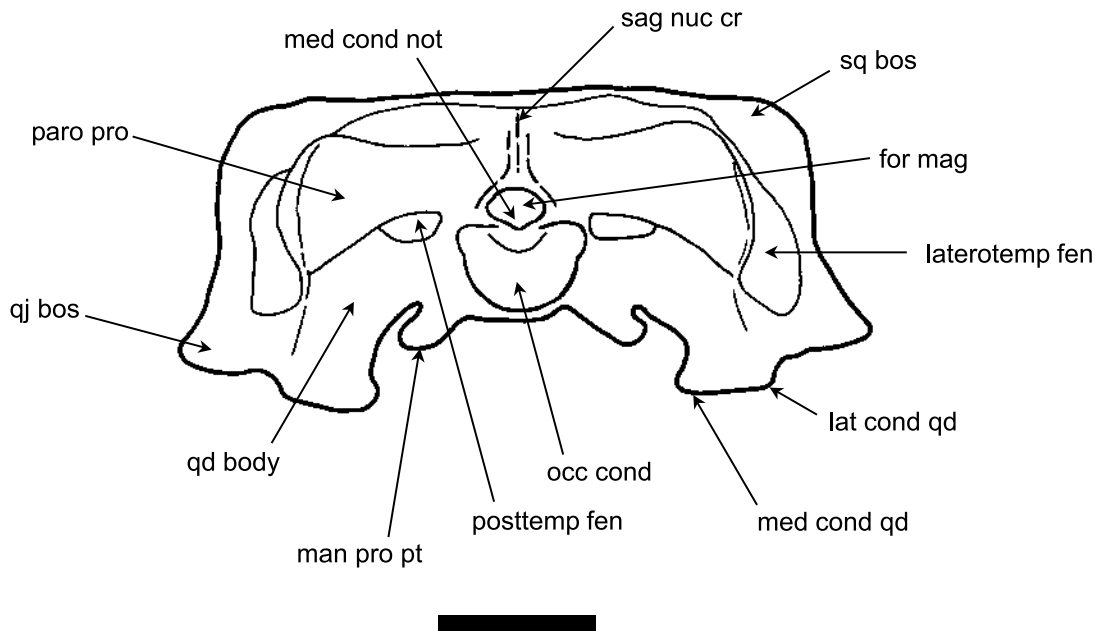
Fig. 5. Ventral view of the braincase and quadrate complex of *Gobisaurus domoculus*, original and interpretive illustration IVPP V12563, holotype. Scale bar represents 100 mm. bas tub, basal tubera; bpt pro, basiptyergoid process; intpt vac, interptyergoid vacuity; lat cond qd, lateral condyle of the quadrate; laterotemp fen, laterotemporal fenestra; man pro pt, mandibular process of the pterygoid; med cond qd, medial condyle of the quadrate; occ cond, occipital condyle; paro pro, paroccipital process; posttemp fen, posttemporal fenestra; qd body, body of the quadrate; qd pro pt, quadrate process of the pterygoid; qd pro qj, quadrate process of the quadratojugal; qj bos, quadratojugal boss; pt body, main body of the pterygoid; suborb fen, suborbital fenestra.



Poor preservation of the basicranium (Figs. 2B, 2D, 5, 6) precludes the identification of certain features. None of the foramina for cranial nerves are evident, and the sutures between individual elements are fused and completely obliterated. Furthermore, the parasphenoid rod (presphenoid rod; Coombs 1971) is not visible within the interptyergoid vacuity. However, the basiptyergoid processes are well preserved and are thick, robust, and anterolaterally oriented. The basal

tubera are present as longitudinal crests. The ventral surface of the basicranium is square in outline and inclined posterodorsally, except for a horizontally oriented convex crest that joins the neck of the occipital condyle. In lateral view, the ventral surface of the basicranium is sellar. The massive occipital condyle (80 mm wide by 44 mm high) is reniform in occipital view, ventrally directed, and offset from the basicranium by a short neck. The dorsal surface of

Fig. 6. Occipital view of the cranium of *Gobisaurus domoculus*, interpretive illustration IVPP V12563, holotype. Scale bar represents 100 mm. for mag, foramen magnum; med cond not, median condylar notch; sag nuc cr, sagittal nuchal crest. Other abbreviations as in Figs. 3 and 5.



the occipital condyle bears a small, sagittally oriented furrow, the median condylar notch. The foramen magnum is ovoid, with a rugose shelf of bone roofing its dorsal surface, directing the opening posteriorly and slightly ventrally.

The paroccipital process (maximal width for the pair 282 mm) curves posteriorly and ventrally (Fig. 2D, 6). A rugose muscle scar caps the distalmost edge of the paroccipital process and continues ventrally along the lateral border of the quadrate. The posttemporal fenestra is visible ventral to the paroccipital processes.

None of the sutures defining the supraoccipital are visible (Figs. 2D, 6). The area between the skull table and the basicranium is rugose and pitted, and there is a narrow sagittal nuchal ridge.

Phylogenetic relationships

To determine the phylogenetic position of *Gobisaurus* within the Ankylosauria, a cladistic analysis involving 22 ankylosaurs (including *Gobisaurus*) and two outgroups was undertaken. All the taxa were selected on the presence of cranial material. Due to their fragmentary nature, *Amtosaurus magnus*, *Maleevus disparoserratus*, and *Niobrarsaurus coleii* were omitted from the analysis. The two outgroups are *Lesothosaurus diagnosticus*, a basal ornithischian, and *Huayangosaurus taibaii*, a basal stegosaur. All suprageneric taxonomic nomenclature follows the definitions of Sereno (1998). Characters selected for the analysis are adapted (except for characters 10 and 32) and modified from previously published sources (Appendix 1). Modifications to terminology have been made, where necessary, to improve clarity and precision, enabling a more extensive array of taxa to be effectively and accurately coded.

Continuously variable (mensural) characters pose problems for character state designation, as the demarcation points are

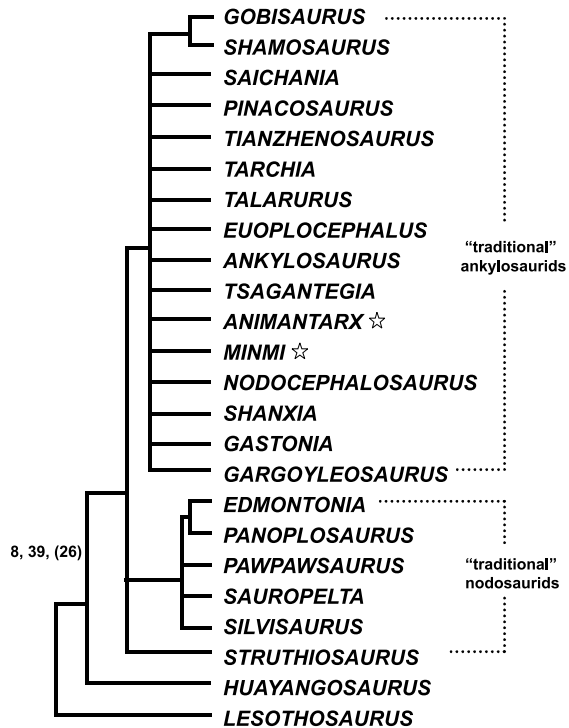
essentially arbitrary. Previously, however, such characters have been extensively employed in ankylosaur systematics and are similarly applied herein. In the case of such characters, precise and (or) relative statements of proportion have been given whenever possible, and coding has been applied accordingly. While a number of original and cast specimens were consulted (Appendix 2), published descriptions, illustrations and photographs were also relied upon to identify character states in many taxa. All characters were effectively re-coded.

Additionally, systematic evaluation of ankylosaur cranial material is burdened with identifying the effects of taphonomic deformation of a highly unusual head skeleton. Many features, such as a depressed lateral profile, suggest that the material recovered from the fossil record may not accurately portray the skeletal morphology as it existed in life. We have tried to lessen erroneous interpretation of cranial features through the examination of multiple specimens (where possible) and by endeavouring to identify taphonomically induced deformation. The resulting data matrix (Appendix 3) was analyzed using the heuristic search algorithm of Phylogenetic Analysis Using Parsimony (PAUP) 3.1.1 (Swofford 1993).

Results and discussion

Analysis of the data matrix resulted in 20 065 equally most parsimonious cladograms of 126 steps (consistency index (CI) = 0.405; retention index (RI) = 0.691; re-scaled consistency index (RC) = 0.280). A strict consensus tree is presented in Fig. 7. Although largely unresolved, this analysis results in a novel genealogical position for both *Animantarx ramaljonensis* (i.e., within the Ankylosauridae; contra Carpenter et al. 1999) and *Struthiosaurus transylvanicus* (as a member of the basal polychotomy defining the Ankylosauria). In addition, this hypothesis supports the notion of *Minmi* sp. as

Fig. 7. A strict consensus tree of the 20,065 most parsimonious cladograms (126 steps each) illustrating the hypothesized genealogy of the Ankylosauria based on cranial evidence. For each taxon, unambiguous (“unequivocal”) characters are followed by ambiguous (“equivocal”) characters in brackets. Presence of a dash (“-”) symbol prior to a character indicates the reversal of the character; an asterisk (“**”) indicates an apomorphy that may represent a more inclusive clade. *Gobisaurus*: (-5); *Shamosaurus*: 1, 8, -30, (-14, -27); *Edmontonia*: 27, 36; *Panoplosaurus*: -5, 11. The open five-pointed star symbol indicates these taxa have previously been considered members of the Nodosauridae, contra the findings presented here (see text for details).

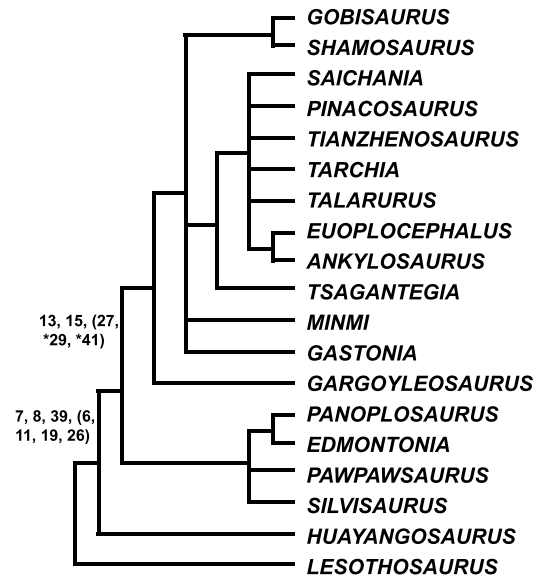


an ankylosaurid (Sereno 1998, 1999; contra Molnar 1980; Coombs and Maryanska 1990). However, as the scope of this analysis was restricted to aspects of the cranium, these statements await subsequent testing.

Incomplete preservation prevented a large number of taxa from being effectively coded for many of the characters. To examine the effect that these taxa had on the phylogenetic hypothesis, two additional analyses were conducted: the first included only those taxa coded for greater than 55% of the characters; the second included only those taxa coded for greater than 80% of the characters. For the first analysis, *Shanxia tianzhensis* (24.4%), *Nodocephalosaurus kirtlandensis* (36.6%), *Struthiosaurus* (36.6%), *Animantarx* (41.6%), and *Sauropelta edwardsi* (51.2%) were eliminated. A total of 54 cladograms of 120 steps was generated (CI = 0.425; RI = 0.673; RC = 0.286). A strict consensus tree (Fig. 8) illustrates the following points of agreement:

- (1) The Ankylosauria is monophyletic, as defined by three unambiguous characters (quadratojugal boss present (character 7); amorphous antorbital cranial ornamentation (character 8); quadrate-paroccipital process fused (character 39)) and four ambiguous characters

Fig. 8. A strict consensus tree of the 54 most parsimonious cladograms (120 steps each) illustrating the hypothesized genealogy of the Ankylosauria based on cranial evidence produced by eliminating *Animantarx*, *Nodocephalosaurus*, *Sauropelta*, *Shanxia*, and *Struthiosaurus* (taxa coded for less than 55% of the available characters). *Gobisaurus*: (-5); *Shamosaurus*: 1, 8, -14, -30, (-27); *Euoplocephalus*: 18; *Ankylosaurus*: 9, -23, -27, 39; *Tsagantegia*: 20, 31, 33, (5, -27); *Gargoyleosaurus*: -19, 22; *Edmontonia*: 27, 36; *Panoplosaurus*: -5, (11); *Huayangosaurus*: 38.



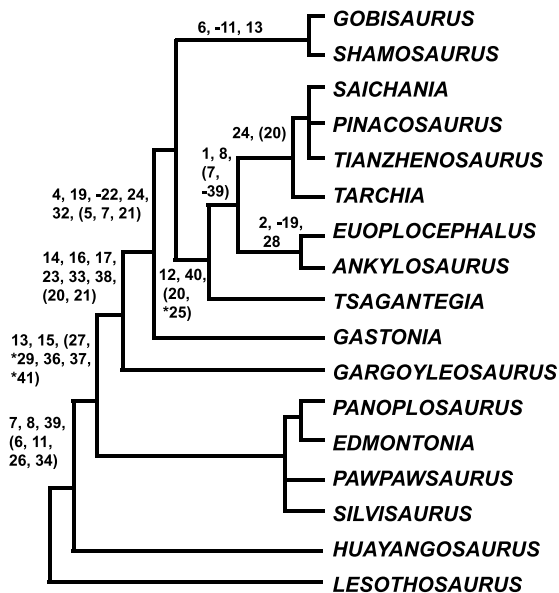
(squamosal boss present (character 6); raised nuchal sculpturing present (character 11); maxillary teeth with cingulum (character 19); paranasal sinus cavities present (character 26)).

- (2) The Ankylosauridae is monophyletic, as defined by two unambiguous characters (premaxillary palate wider than long (character 13); premaxillary notch present (character 15)) and three ambiguous characters (anterior face of pterygoid vertically or anteriorly inclined (character 27); mandibular process of the pterygoids directed anterolaterally (character 29); postocular shelf present (character 41)).
- (3) *Shamosaurus* and *Gobisaurus* are sister taxa.
- (4) *Tsagantegia* is the sister taxon of the remaining ankylosaurines.
- (5) *Ankylosaurus* and *Euoplocephalus* are sister taxa.
- (6) *Edmontonia* and *Panoplosaurus* are sister taxa.

The third analysis further eliminated *Minmi* sp. (Molnar 1996; 56.1%) and *Talarurus plicatospineus* (58.5%). Six equally most parsimonious trees of 114 steps were generated (CI = 0.447; RI = 0.682; RC = 0.305). A strict consensus tree is given in Fig. 9. While this hypothesis is considerably better resolved than the previous cladograms (Figs. 7, 8), it is consistent with the genealogical affinities proposed by the second analysis.

All three cladograms (Figs. 7–9) illustrate the following congruent statements: (1) the Ankylosauria is monophyletic; (2) *Shamosaurus* and *Gobisaurus* are sister taxa; and (3) *Edmontonia* and *Panoplosaurus* are sister taxa. Furthermore, sequential examination of these hypotheses supports the notion that the elimination of poorly coded taxa may

Fig. 9. A strict consensus tree of 6 most parsimonious cladograms (114 steps each) illustrating the hypothesized genealogy of the Ankylosauria based on cranial evidence produced by eliminating *Minmi* and *Talarurus*, in addition to those removed from Fig. 8 (*Animantarx*, *Nodocephalosaurus*, *Sauropelta*, *Shanxia*, and *Struthiosaurus*; taxa coded for less than 80% of the available characters). *Gobisaurus*: (-5); *Shamosaurus*: 1, 8, -14, -30, (27); *Tarchia*: -36, (20); *Euoplocephalus*: 18; *Ankylosaurus*: 9, -23, (27, 39); *Tsagantegia*: -31, -33, -36, (5, 27); *Gastonia*: 2, 28, -30, (34); *Gargoyleosaurus*: 22; *Edmontonia*: 27, 36; *Panoplosaurus*: -5, (11); *Huayangosaurus*: 38.



increase the potential resolution of a phylogenetic hypothesis (although see Wu et al. 1996 for contradictory results).

A question of generic segregation?

The absence of antorbital and dorsotemporal fenestrae, the complete obliteration of most of the cranial sutures, and the presence of cranial ornamentation across the dorsum clearly characterize *Gobisaurus* as a member of the Ankylosauria. *Gobisaurus* may further be assigned to the clade Ankylosauridae, based on the presence of a premaxillary notch (character 15). Systematic evaluation of ankylosaur cranial material (see above) places *Gobisaurus* as the sister taxon of *Shamosaurus scutatus* (Tumanova 1985) nested within the Ankylosaurinae as one of several successive outgroups of the Ankylosaurinae (Figs. 7–9).

Shamosaurus, from the Early Cretaceous (Aptian–Albian) of Mongolia and *Gobisaurus* share a similar temporal and geographic distribution (Fig. 1), in addition to demonstrating a number of congruent morphological features. Included amongst these are a delta-shaped dorsal profile; a narrow premaxillary rostrum; rounded squamosal and quadratojugal bosses; and large and prominent rostrally oriented orbits and external nares (in *Shamosaurus*, the orbits and external nares represent approximately 18% and 19%, respectively, of the overall cranial length). Previous taxonomic work on ankylosaurs suggests that concordant morphology and overlapping temporal–geographic distribution are unremarkable

amongst members of this clade (e.g., *Edmontonia* and *Panoplosaurus*; see Carpenter 1990). Both *Shamosaurus* and *Gobisaurus* may be diagnosed by a suite of unique apomorphic and plesiomorphic character state combinations (Appendix 3). Furthermore, each taxon may be defined on the basis of one or more autapomorphies (*Shamosaurus* reportedly has a maxillary tooth row approximately 50% of the overall cranium length (Tumanova 1983; Coombs and Maryanska 1990); *Gobisaurus* has elongate premaxillary processes of the vomers visible in palatal view).

A recent debate concerning the legitimacy of the ankylosaurid genera *Shanxia* and *Tianzhenosaurus* (see Upchurch and Barrett 2000; Sullivan 2000) underscores the issue of establishing new taxa based on limited osteological evidence, particularly in the absence of a substantial systematic evaluation. Using this rationale, the validity of *Shanxia* does appear to be questionable, predicated upon the non-unique distribution of character states (Appendix 3). However, the status of the synonymy of *Tianzhenosaurus* and *Saichania* (Sullivan 1999; 2000) is less conclusive. The present study indicates that *Tianzhenosaurus* is diagnosed by a unique combination of character states, although it remains uncertain (owing to the vagueness of the literature; see Pang and Cheng 1998) whether or not the taxon is defined by autapomorphies.

Given the dearth of material generally ascribed to a particular fossil taxon, coupled with the potential for intrataxon variation, estimation of generic (or specific) segregation is often a perilous systematic endeavour. Our analyses clearly cluster *Gobisaurus* and *Shamosaurus* as sister taxa, an assignment that intuitively draws attention to the strength of the dichotomy. However, the degree of morphological discrepancy that has been noted, together with our current understanding of ankylosaur biology, supports the conclusion that *Gobisaurus* is phylogenetically distinct at a generic level.

Acknowledgments

The authors wish to thank Drs. X.-C. Wu (Canadian Museum of Nature, Ottawa, Ontario), S. Modesto (Royal Ontario Museum, Toronto, Ontario), O.R.P. Bininda-Emonds (Leiden University, Leiden, The Netherlands), and Messrs. R.V. Hill (State University of New York, Stony Brook, N.Y.) and D. Bininda (University of Calgary, Calgary, Alberta) for providing assistance in generating the phylogenetic analysis. Drs. H.-D. Sues (Royal Ontario Museum, Toronto), P.M. Galton (University of Bridgeport, Connecticut), K. Carpenter (Denver Museum of Nature and Science, Denver, Colorado), Ms. L. McGregor and Messrs. W. Fitch and E. Snively (University of Calgary) reviewed the paper and made significant improvements to the text. This research was supported by a Heaton Student Support Grant (TMP) awarded to MKV and a Natural Sciences and Engineering Research Council Operating Grant (OGP 0009745) awarded to APR.

References

Barrett, P.M., Hailu, Y., Upchurch, P., and Burton A.C. 1998. A new ankylosaurian dinosaur (Ornithischia: Ankylosauria) from

- the Upper Cretaceous of Shanxi Province, People's Republic of China. *Journal of Vertebrate Paleontology*, **18**: 376–384.
- Baumel, J.J., King, A.S., Breazile, J.E., Evans, H.E., and Vanden Berge, J.C. (Editors). 1993. *Handbook of Avian Anatomy: Nomina Anatomica Avium*. 2nd Ed. Publications of the Nuttall Ornithological Club, No. 23. Cambridge, Massachusetts.
- Brown, B. 1908. The Ankylosauridae, a new family of armored dinosaurs from the Upper Cretaceous. *Bulletin of the American Museum of Natural History*, **24**: 187–201.
- Carpenter, K. 1990. Ankylosaur systematics: example using *Panoplosaurus* and *Edmontonia* (Ankylosauria: Nodosauridae). In *Dinosaur systematics: approaches and perspectives*. Edited by K. Carpenter and P.J. Currie. Cambridge University Press, Cambridge, pp. 281–298.
- Carpenter, K., and Kirkland, J.I. 1998. Review of Lower and Middle Cretaceous ankylosaurs from North America. *Lower and Middle Cretaceous Terrestrial Ecosystems*, New Mexico Museum of Natural History and Science Bulletin **14**: 249–270.
- Carpenter, K., Miles, C., and Cloward, K. 1998. Skull of a Jurassic ankylosaur (Dinosauria). *Nature (London)*, **393**: 782–783.
- Carpenter, K., Kirkland, J.I., Burge, D., and Bird, J. 1999. Ankylosaurs (Dinosauria: Ornithischia) of the Cedar Mountain Formation, Utah, and their stratigraphic distribution. In *Vertebrate paleontology in Utah*. Utah Geological Survey, Miscellaneous Publication 99–1, pp. 243–251.
- Coombs, W.P., Jr. 1971. The Ankylosauria. Ph.D. thesis, Columbia University, New York.
- Coombs, W.P., Jr. 1978. The families of the ornithischian dinosaur order Ankylosauria. *Palaeontology*, **21**: 143–170.
- Coombs, W.P., Jr., and Maryanska, T. 1990. Ankylosauria. In *The Dinosauria*. Edited by D.B. Weishampel, P. Dodson, and H. Osmólska. University of California Press, Berkeley, Calif., pp. 456–483.
- Currie, P.J. 1997. Sino-Soviet Expeditions. In *Encyclopedia of dinosaurs*. Edited by P.J. Currie and K. Padian. Academic Press, New York, pp. 661–662.
- Eaton, T.H., Jr. 1960. A new armored dinosaur from the Cretaceous of Kansas. *University of Kansas Paleontological Contribution*, **25**: 1–24.
- Galton, P.M. 1990. Stegosauria. In *The Dinosauria*. Edited by D.B. Weishampel, P. Dodson, and H. Osmólska. University of California Press, Berkeley, Calif., pp. 435–455.
- Gilmore, C.W. 1923. A new species of *Corythosaurus* with notes on other Belly River Dinosauria. *Canadian Field-Naturalist*, **37**: 46–52.
- Gilmore, C.W. 1930. On dinosaurian reptiles from the Two Medicine Formation of Montana. *Proceedings of the United States National Museum*, **77**: 1–39.
- Gilmore, C.W. 1933. On the dinosaurian fauna of the Iren Dabasu Formation. *Bulletin of the American Museum of Natural History*, **67**: 23–78.
- Hill, R.V. 1999. Phylogenetic relationships among Ankylosauria: an analysis of cranial characters. *Journal of Vertebrate Paleontology* **19** (supplement to No. 3): 51A.
- Hu, S.-Y. 1964. Carnosaurian remains from Alshan, Inner Mongolia. *Vertebrata Palasiatica*, **8**: 42–63.
- Kirkland, J.I. 1998. A polacanthine ankylosaur (Ornithischia: Dinosauria) from the Early Cretaceous (Barremian) of eastern Utah. *Lower and Middle Cretaceous Terrestrial Ecosystems*, New Mexico Museum of Natural History and Science Bulletin, **14**: 271–281.
- Lee, Y.-N. 1996. A new nodosaurid ankylosaur (Dinosauria: Ornithischia) from the Paw Paw Formation (Late Albian) of Texas. *Journal of Vertebrate Paleontology*, **16**: 232–245.
- Maryanska, T. 1971. New data on the skull of *Pinacosaurus grangeri* (Ankylosauria). *Palaeontologica Polonica*, **25**: 45–53.
- Maryanska, T. 1977. Ankylosauridae (Dinosauria) from Mongolia. *Palaeontologica Polonica*, **37**: 85–151.
- Molnar, R.E. 1980. An ankylosaur (Ornithischia: Reptilia) from the Lower Cretaceous of southern Queensland. *Memoirs of the Queensland Museum*, **20**: 77–87.
- Molnar, R.E. 1996. Preliminary report of a new ankylosaur from the Early Cretaceous of Queensland, Australia. *Memoirs of the Queensland Museum*, **39**: 653–668.
- Pang, Q., and Cheng, Z. 1998. A new ankylosaur of Late Cretaceous from Tianzhen, Shanxi. *Progress in Natural Science*, **8**: 326–334.
- Pereda-Suberbiola, J., and Galton, P.M. 1994. A revision of the cranial features of the dinosaur *Struthiosaurus austriacus* Bunzel (Ornithischia: Ankylosauria) from the Late Cretaceous of Europe. *Neues Jahrbuch für Geologie und Paläontologie Abh.*, **191**: 173–200.
- Pereda-Suberbiola, X., and Galton, P.M. 1997. Armoured dinosaurs from the Late Cretaceous of Transylvania. *Acta Musei Devensis, Sargetia, Series Scienta Naturae*, **17**: 203–217.
- Russell, L.S. 1940. *Edmontonia rugosidens* (Gilmore) an armored dinosaur from the Belly River Series of Alberta. *University of Toronto Studies, Geology Series*, **43**: 1–28.
- Sereno, P.C. 1986. Phylogeny of the bird-hipped dinosaurs (Order Ornithischia). *National Geographic Research*, **2**: 234–256.
- Sereno, P.C. 1991. *Lesothosaurus*, “fabrosaurids,” and the early evolution of Ornithischia. *Journal of Vertebrate Paleontology*, **11**: 168–197.
- Sereno, P.C. 1998. A rationale for phylogenetic definitions, with application to the higher-level taxonomy of Dinosauria. *Neues Jahrbuch für Geologie und Paläontologie Abh.*, **210**: 41–83.
- Sereno, P.C. 1999. The evolution of dinosaurs. *Science*, **284**: 2137–2147.
- Sereno, P.C., and Zhimin, D. 1992. The skull of the basal stegosaur *Huayangosaurus taibaii* and a cladistic analysis of the Stegosauria. *Journal of Vertebrate Paleontology*, **12**: 318–343.
- Sternberg, C.M. 1929. A toothless armoured dinosaur from the Upper Cretaceous of Alberta. *National Museum of Canada Bulletin*, **54**: 28–33.
- Sullivan, R.M. 1999. *Nodocephalosaurus kirtlandensis*, gen. et sp. nov., a new ankylosaurid dinosaur (Ornithischia: Ankylosauria) from the Upper Cretaceous Kirtland Formation (Upper Campanian), San Juan Basin, New Mexico. *Journal of Vertebrate Paleontology*, **19**: 126–139.
- Sullivan, R.M. 2000. Reply to Upchurch and Barrett. *Journal of Vertebrate Paleontology*, **20**: 218–219.
- Swofford, D.L. 1993. PAUP: Phylogenetic Analysis Using Parsimony, version 3.1.1. Computer software and documentation distributed by Illinois Natural History Survey, Champaign, Illinois.
- Tumanova, T.A. 1977. New data on the ankylosaur *Tarchia gigantea*. *Paleontological Zhurnal*, **1977**: 92–100. (In Russian.)
- Tumanova, T.A. 1983. The first ankylosaur from the Lower Cretaceous of Mongolia. *Sovmestnaya Sovetsko-Mongol'skaya Paleontogicheskaya Ekpeditsiya, Trudy*, **24**: 110–120. (In Russian with English summary.)
- Tumanova, T.A. 1985. Skull morphology of the ankylosaur *Shamosaurus scutatus* from the Lower Cretaceous of Mongolia. In *Les Dinosauriens de la Chine à la France*. Edited by P. Taquet and C. Sudre. *Museum d'Histoire Naturelle de Toulouse, France and Museum d'Histoire Naturelle, Chongqing, People's Republic of China*, pp. 73–79.
- Tumanova, T.A. 1987. The armored dinosaurs of Mongolia. *Sovmestnaya Sovetsko-Mongol'skaya Paleontogicheskaya Ekpeditsiya, Trudy* **32**: 1–80. (In Russian with English summary.)

- Tumanova, T.A. 1993. A new armored dinosaur from south-eastern Gobi. *Paleontological Journal*, **27**: 119–125.
- Upchurch, P., and Barrett, P.M. 2000. The taxonomic status of *Shanxia tianzhenensis* (Ornithischia, Ankylosauridae); response to Sullivan (1999). *Journal of Vertebrate Paleontology*, **20**: 216–217.
- Vickaryous, M.K., Russell, A.P., and Currie, P.J. 2001. The cranial ornamentation of ankylosaurs (Ornithischia: Thyreophora): reappraisal of developmental hypotheses. In *The armored dinosaurs*. Edited by K. Carpenter. Indiana University Press, Bloomington, Ind., pp. 318–340.
- Weishampel, D.B., and Witmer, L.M. 1990. *Lesothosaurus*, *Pisanosaurus*, and *Technosaurus*. In *The Dinosauria*. Edited by D.B. Weishampel, P. Dodson, and H. Osmólska. University of California Press, Berkeley, Calif., pp. 416–425.
- Weishampel, D.B., Grigorescu, D., and Norman, D.B. 1991. The dinosaurs of Transylvania. *National Geographic Research and Exploration*, **7**: 196–215.
- Wu, X.-C., Brinkman, D.B., and Russell, A.P. 1996. A new alligator from the Upper Cretaceous of Canada and the relationships of early eusuchians. *Palaeontology*, **39**: 351–375.
8. Cranial ornamentation in a transverse plane across the antorbital region: absent (0); present, amorphous–ill-defined (1); present, distinct pattern of sculpturing consists of three or more flat polygons (2); present, distinct pattern of sculpturing consists of three or more bulbous polygons (3); present, distinct pattern of sculpturing consists of one or two flat polygons (4) (Coombs 1978; Kirkland 1998; Hill 1999; Sereno 1999). The pattern and morphology of ectopic intramembranous ossifications (e.g., osteoderms) coalesced to the dorsal surface of the head skeleton proper (sensu Vickaryous et al. 2001); generally best developed across the antorbital region.
9. Shallow furrows demarcate a single area of cranial ornamentation between the external nares: absent (0); present (1) (Coombs 1978; Kirkland 1998).
10. Skull table morphology: width between squamosals greater than or equal to width between supraorbitals (0); width between squamosals less than width between supraorbitals (1) (new). The skull table refers to the area bounded by a transverse plane between the lateralmost points of the squamosals and a transverse plane between the lateralmost points of the supraorbitals.
11. Raised nuchal sculpturing: absent (0); present (1) (Kirkland 1998; Hill 1999). A localized pattern of cranial ornamentation running transversely across the dorso-occipital surface of the parietals.
12. Nuchal shelf: does not obscure occiput in dorsal view (0); obscures occiput in dorsal view (1) (Coombs 1978; Barrett et al. 1998; Carpenter et al. 1998; Kirkland 1998; Hill 1999). The nuchal shelf represents a posterior extension of the parietals and possibly several cossified osteoderms that may shelter the occiput (paroccipital processes, occipital condyle) in dorsal view.

Appendix 1.

Table A1. List of characters used in this study.

Dermatocranium, external surface

1. Maximum cranial dimension: cranium length greater than cranial width (0); cranial width equal to or greater than cranial length (1) (Coombs 1978; Coombs and Maryanska 1990; Tumanova 1987; Barrett et al. 1998; Kirkland 1998; Hill 1999; Sereno 1999). Maximum cranial length was determined by measuring the overall distance from the anteriormost tip of the premaxillary rostrum sagittally along the palatal surface to the posteriormost edge of the occipital condyle. Maximum cranial width was determined by measuring the distance (across the palatal surface) between the lateralmost edges of the quadratojugals. In taxa where the quadratojugals project far ventrally, careful attention was given to the estimation of cranial width, attempting to identify any taphonomic distortion.
2. Cranial roof in lateral profile anterior to orbits: flat (0); dome-like (1) (Lee 1996; Carpenter et al. 1998; Sereno 1999).
3. Cranial roof in lateral profile posterior to orbits: flat (0); dome-like (1) (Lee 1996; Hill 1999).
4. Laterotemporal fenestrae in lateral view: visible (0); not visible (1) (Coombs 1978; Tumanova 1987; Carpenter et al. 1998; Kirkland 1998; Hill 1999).
5. Supraorbital boss: absent (0); present, rounded protuberance, laterally oriented (1); present, longitudinal ridge, dorsolaterally oriented (2) (Sereno 1986; Lee 1996; Hill 1999).
6. Squamosal boss: absent (0); present, rounded protuberance (1); present, pyramidal protuberance (2) (Coombs 1978; Tumanova 1987; Sereno 1986, 1999; Barrett et al. 1998; Carpenter et al. 1998; Kirkland 1998; Hill 1999).
7. Quadratojugal boss: absent (0); present, rounded protuberance (1); present, delta-shaped protuberance (2) (Coombs 1978; Tumanova 1987; Sereno 1986, 1999; Barrett et al. 1998; Kirkland 1998; Hill 1999).

Palate

13. Maximum premaxillary rostrum dimension: premaxillary palate length equal to or greater than premaxillary palate width (0); premaxillary palate length less than premaxillary palate width (1) (Kirkland 1998; Hill 1999; Sereno 1999). Maximum premaxillary palate length was determined by measuring the distance (sagittal plane along the palatal surface) between a the midpoint of a line extended between the medial edges of the anteriormost tomial crests and the midpoint of a line extended between the anteriormost maxillary teeth. Premaxillary palate width was determined by measuring the maximum transverse distance between the medial surface of the tomia and (or) premaxillary teeth.
14. Maximum premaxillary rostrum width: less than the distance between the posteriormost maxillary teeth (0); equal to or greater than the distance between the posteriormost maxillary teeth (1) (Tumanova 1987; Kirkland 1998). Premaxillary rostrum width was determined by measuring the transverse distance between the lateral surfaces of the premaxillae at their maximum. The distance between the posteriormost maxillary teeth was determined by

measuring the transverse distance between the lateral surfaces of the tooth rows.

15. Premaxillary notch: absent (0); present (1) (Kirkland 1998; Hill 1999; Sereno 1999).
A small inverted V- or U-shaped opening at the anteriormost point between opposing premaxillary tomia.
16. Premaxillary tomia: restricted to an extreme anterior position (0); extend posteriorly, continuous with maxillary tooth row (1); extends posteriorly, lateral to maxillary tooth row (2) (Carpenter et al. 1998; Hill 1999; Sereno 1999).
17. Premaxillary teeth: present (0); absent (1) (Coombs and Maryanska 1990; Carpenter et al. 1998; Kirkland 1998; Hill 1999; Sereno 1999).
18. Maxillary tooth rows: straight, converge anteriorly (0); curved into an hourglass-shape, converge and then diverge (1) (Coombs 1978; Coombs and Maryanska 1990; Sereno 1986; 1999; Lee 1996; Carpenter et al. 1998; Kirkland 1998; Hill 1999).
19. Maxillary tooth cingulum: absent (0); present (1) (Coombs 1978; Kirkland 1998; Hill 1999; Sereno 1999).
20. Vomers: incomplete, not bisecting the rostrum longitudinally (0); complete, bisecting the rostrum longitudinally (1) (Sereno 1986; 1999; Coombs and Maryanska 1990; Lee 1996; Carpenter et al. 1998; Hill 1999).
21. Secondary palate: absent (0); anterodorsal palatal arch only (1); anterodorsal and posteroventral palatal arches (2) (Coombs 1978; Sereno 1986; Tumanova 1987; Coombs and Maryanska 1990; Lee 1996; Carpenter et al. 1998; Kirkland 1998).
In ankylosaurs, the secondary palate is made up of variable contributions from the maxillae, vomers, and palatines (Coombs and Maryanska 1990). While in some taxa the secondary palate is restricted to a position anterior to the choanae (essentially extending the premaxillary palate), many ankylosaurs also develop an additional secondary palate posterior to the choanae. This posteroventral secondary palate projects anteriorly from the pterygoid complex and reduces the diameter of the choanae. As a result, air passing in a net posterior direction through the nasal cavity moves over the anterodorsal secondary palate and then undulates anteriorly and then ventrally over the posteroventral secondary palate (Coombs 1978).
22. Buccal emargination: flat (0); strongly concave (1) (Coombs 1978; Sereno 1986; Lee 1996).

Respiratory passageways

23. External nares proper: not visible in anterior view (0); visible in anterior view (1) (Tumanova 1987; Carpenter et al. 1998; Kirkland 1998; Hill 1999).
24. Narial septum: absent (0); present, horizontal (1); present, vertical (2) (Hill 1999; Sereno 1999).
25. Nasal cavity proper: relatively linear orientation (0); convoluted (1) (Coombs 1978; Tumanova 1987; Kirkland 1998; Hill 1999; Sereno 1999).
Fortuitous broken specimens, physical sectioning, and non-invasive CT revealed these conditions.
26. Paranasal sinus cavities: absent (0); present (1) (Coombs 1978; Tumanova 1987; Sereno 1986, 1999; Carpenter et al. 1998; Hill 1999).

Fortuitous broken specimens, physical sectioning, and non-invasive CT have revealed blind-ended sinus cavities in some ankylosaur taxa. While these sinuses have generally been associated with the presence of narial septa, the nature of this relationship remains to be assessed. A recently prepared specimen of *Edmontonia rugosidens* (TMP 98.71.1) indicates that members of this taxon do possess premaxillary sinus cavities, a feature previously unrecorded in the literature.

Pterygoid complex, braincase, and occiput

27. Anterior face of pterygoid body: directed posteriorly (0); directed vertically or anteriorly (1) (Tumanova 1987; Sereno 1999).
The body of the pterygoid complex forms a transverse partition between the palate and the braincase. Moving ventrally, the anterior face of this partition may be directed either towards the occiput or vertically.
28. Posterior margin of the pterygoid: anterior to (0); or in transverse alignment with (1) the ventral margin of the pterygoid process of the quadrate (Lee 1996; Sereno 1999).
29. Mandibular ramus of the pterygoid: directed parasagittally (0); anterolaterally (1) (Coombs 1978).
30. Basipterygoid process – pterygoid contact: fused (0); unfused (1) (Coombs 1978; Tumanova, 1987; Sereno 1999).
31. Basisphenoid length: greater than basioccipital length (0); less than basioccipital length (1) (Sereno 1986, 1999).
32. Basal tubera: bulbous (0); rugose crests (1) (new)
33. Paroccipital process directed: posterolaterally (0); laterally (1) (Tumanova 1987; Carpenter et al. 1998; Hill 1999).
34. Occipital condyle: composed of multiple elements (0); composed of basioccipital only (1) (Sereno 1986, 1999; Kirkland 1998; Hill 1999).
35. Occipital condyle morphology in occipital view: reniform (0); ovoid-round (1) (Sereno 1986; 1999; Tumanova 1987; Coombs and Maryanska 1990; Lee 1996; Carpenter et al. 1998; Hill 1999).
36. Occipital condyle directed: directly posteriorly (0); posteroventrally (1) (Sereno 1986; Kirkland 1998; Hill 1999).
37. Foramen magnum: directed posteriorly (0); directed posteroventrally (1) (Coombs 1978).

Quadrate

38. Quadrate lateral profile: bowed, anteriorly convex, posteriorly concave (0); flat (1) (Hill 1999).
39. Quadrate – paroccipital process contact: unfused (0); fused (1) (Tumanova 1987; Coombs and Maryanska 1990; Lee 1996; Carpenter et al. 1998; Hill 1999).
40. Quadrate condyle, lateral view: visible (0); obscured by the quadratojugal (1) (Tumanova 1987).

Other

41. Postocular shelf (jugal–postorbital): absent (0); present (1) (Coombs 1978; Coombs and Maryanska 1990; Sereno 1986, 1999; Barrett et al. 1998).

Appendix 2

Table A2. Cranial material examined during the course of this study.

Taxon	Specimen(s)	Source(s)
<i>Animantarx</i>	CEUM 6228R*	Carpenter et al. 1999
<i>Ankylosaurus</i>	AMNH 5895*; AMNH 5214; NMC 8880	Brown 1908; Coombs 1978; Coombs and Maryanska 1990
<i>Edmontonia</i>	NMC 8531 ^a ; AMNH 3076 ^a ; AMNH 5381 ^a ; AMNH 5665 ^a ; TMP 98.71.1 ^a ; cast of USNM 11868 ^b	Gilmore 1930; Carpenter 1990; Coombs and Maryanska 1990
<i>Euoplocephalus</i>	NMC 0210*; AMNH 5337; AMNH 5405; NMC 8530; NMC 8876; TMP 91.127.1; TMP 97.59.1; TMP 97.132.1; UALVP 31	Gilmore 1923; Sternberg 1929; Coombs 1971, 1990; Coombs and Maryanska 1990;
<i>Gargoyleosaurus</i>	DMNH 27726*	Carpenter et al. 1998
<i>Gastonia</i>	CEUM 1307*	Kirkland, 1998
<i>Gobisaurus</i>	IVPP V12563*	This study
<i>Minmi</i>	None	Molnar 1996; Coombs and Maryanska 1990
<i>Nodocephalosaurus</i>	None	Sullivan 1999
<i>Panoplosaurus</i>	NMC 2759*; TMP 83.25.2	Russell 1940; Carpenter 1990; Coombs and Maryanska 1990
<i>Pawpawsaurus</i>	Cast of SMU 73203*	Lee 1996; Carpenter and Kirkland 1998
<i>Pinacosaurus</i>	AMNH 6523*; four uncatalogued subadult specimens from the IVPP	Gilmore 1933; Maryanska 1971, 1977; Tumanova 1987; Coombs and Maryanska 1990
<i>Saichania</i>	Cast of GI SPS 100/151	Maryanska 1977; Tumanova 1987; Coombs and Maranska 1990
<i>Sauropelta</i>	AMNH 3035	Coombs and Maryanska 1990; Carpenter and Kirkland 1998
<i>Shamosaurus</i>	None	Tumanova 1985, 1987; Coombs and Maryanska 1990
<i>Shanxia</i>	None	Barrett et al. 1998
<i>Silvisaurus</i>	None	Eaton 1960; Coombs and Maryanska 1990; Carpenter and Kirkland 1998
<i>Struthiosaurus</i>	Cast of BM(NH) R4966	Coombs and Maryanska 1990; Weishampel et al. 1991; Pereda-Suberbiola and Galton 1994, 1997
<i>Talarurus</i>	None	Maryanska 1977; Tumanova 1987; Coombs and Maranska 1990
<i>Tarchia</i>	None	Tumanova 1977, 1987; Coombs and Maryanska 1990
<i>Tianzhenosaurus</i>	None	Pang and Cheng 1998
<i>Tsagantegia</i>	None	Tumanova 1993
<i>Lesothosaurus</i>	None	Weishampel and Witmer 1990; Sereno 1991
<i>Huayangosaurus</i>	None	Galton 1990; Sereno and Zhimin 1992

^aSpecimens referred to the taxon *Edmontonia rugosidens*.

^bSpecimens referred to the taxon *Edmontonia longiceps*.

*Type specimen.

Appendix 3

Table A3. Character state distribution among the 24 taxa considered in this study.

	1	1 1 1 1 1	1 1 1 1 2	2 2 2 2 2	2 2 2 2 3	3 3 3 3 3	3 3 3 3 4	4	%	
	1 2 3 4 5	6 7 8 9 0	1 2 3 4 5	6 7 8 9 0	1 2 3 4 5	6 7 8 9 0	1 2 3 4 5	6 7 8 9 0	1	
<i>Ankylosaurus</i>	1 1 0 1 2	2 2 2 1 0	1 1 1 1 1	2 1 0 0 1	2 1 0 ? 1	1 0 1 1 1	1 1 1 1 0	1 1 1 1 1	1	97.5
<i>Euoplocephalus</i>	1 1 0 1 2	2 2 2 0 0	1 1 1 1 1	2 1 1 0 1	2 1 1 2 1	1 1 1 1 1	1 1 1 1 0	1 1 1 0 1	1	100
<i>Saichania</i>	1 0 0 1 2	2 2 3 0 0	1 1 1 0 1	2 1 0 1 0	2 ? 1 1 1	1 1 0 1 0	1 1 1 1 0	1 1 ? 1 1	1	95
<i>Tarchia</i>	1 0 0 1 2	2 2 2 0 0	1 1 1 1 1	2 1 0 1 1	2 ? 1 1 ?	1 1 0 1 1	1 1 1 1 0	0 1 ? 0 1	?	90.2
<i>Pinacosaurus</i>	1 0 0 1 2	2 2 ? ? 0	? 1 1 1 1	2 1 0 1 0	2 1 1 1 1	1 1 0 1 0	1 1 1 0 0	1 0 ? 0 1	1	90.2
<i>Tsagantegia</i>	0 0 0 1 1	2 1 1 0 0	1 1 1 1 1	2 1 0 1 1	2 ? 1 2 ?	1 0 0 1 1	0 1 0 1 0	0 1 1 1 1	?	92.7
<i>Shamosaurus</i>	1 0 0 1 2	1 1 2 0 0	0 0 0 0 1	2 1 0 ? 1	2 0 1 2 ?	? 0 0 1 0	? 1 ? ? 0	1 ? 1 1 0	1	82.9
<i>Minmi</i>	0 0 0 1 1	2 2 ? ? 0	? 0 ? 0 1	2 0 0 1 ?	? ? ? ? ?	? ? 0 ? ?	1 ? 0 0 0	0 0 1 ? ?	?	54.8
<i>Gargoyleosaurus</i>	0 0 0 0 0	2 2 1 0 1	1 0 1 0 1	0 0 0 0 0	0 1 0 0 0	? 1 0 1 ?	? ? 0 ? 0	? ? 0 1 0	?	80.5
<i>Gastonia</i>	0 1 0 0 0	2 2 1 0 1	1 0 1 1 1	2 1 0 0 ?	1 0 1 0 0	? ? 1 1 0	1 0 1 0 0	1 1 1 ? 0	?	87.8
<i>Edmontonia</i>	0 0 1 0 1	0 1 4 1 1	0 0 0 0 0	1 1 1 1 1	1 0 0 0 0	1 1 1 0 ?	? 1 0 1 1	1 ? 0 1 0	0	92.7
<i>Panoplosaurus</i>	0 0 1 0 0	0 1 4 1 1	1 0 0 0 0	1 1 1 1 ?	1 ? 0 0 ?	? 0 1 0 ?	? 1 0 1 1	0 1 0 1 0	0	85.4
<i>Silvisaurus</i>	0 1 1 0 1	0 1 1 0 1	0 0 0 0 0	0 0 0 1 1	0 0 0 0 ?	? 0 1 0 1	1 0 1 ? 1	0 0 0 1 1	?	87.8
<i>Sauropelta</i>	0 0 1 0 1	0 1 1 ? 1	0 0 ? ? ?	? ? ? 1 ?	? ? ? ? ?	? ? ? ? 1	? 0 0 1 1	1 0 0 ? 0	?	50
<i>Animantax</i>	? 1 0 0 0	1 1 1 ? 1	1 0 ? ? ?	? ? 1 ? ?	? ? ? ? ?	? ? ? ? ?	? 0 ? ? 0	? 0 1 ? 0	1	40.5
<i>Pawpawsaurus</i>	0 0 1 0 1	2 2 1 1 1	1 0 0 0 0	0 0 1 1 0	0 0 0 0 0	0 0 1 0 0	1 0 0 1 1	0 0 0 1 0	?	97.5
<i>Nodocephalosaurus</i>	? 0 0 1 2	2 2 3 1 ?	? ? ? ? ?	? ? ? ? 1	? ? 1 ? ?	1 ? ? ? ?	? 1 ? 1 0	? ? ? ? ?	1	35.7
<i>Talarurus</i>	? 0 0 1 2	2 2 2 ? 0	1 1 ? ? ?	? ? ? ? 1	? ? ? 2 ?	1 1 ? 1 0	1 1 0 1 0	1 ? ? 0 ?	1	58.5
<i>Tianzhenosaurus</i>	1 0 0 1 2	2 2 3 1 0	1 1 1 0 ?	2 1 0 ? 1	? ? 1 0 ?	? ? 0 1 0	0 0 1 0 0	1 1 1 0 1	?	80.5
<i>Gobisaurus</i>	0 0 0 1 0	1 1 1 0 0	0 0 0 1 1	2 1 0 1 1	2 0 1 2 0	1 1 0 1 1	? 1 1 ? 0	1 1 1 1 0	1	95.1
<i>Struthiosaurus</i>	? ? ? 0 0	0 0 ? ? 1	0 0 ? ? ?	? ? ? ? ?	? ? ? ? ?	? ? ? ? ?	? ? 0 1 0	0 0 1 1 0	?	35.7
<i>Shanxia</i>	? ? 0 ? ?	? 2 ? ? ?	1 1 ? ? ?	? ? ? ? ?	? ? ? ? ?	? ? ? ? ?	? 1 1 1 0	1 1 ? ? ?	?	21.4
<i>Lesothosaurus</i>	0 0 0 0 0	0 0 0 0 0	0 0 0 0 0	0 0 0 0 0	0 ? ? 0 0	0 0 0 ? 1	0 1 0 0 0	0 0 0 0 0	0	92.6
<i>Huayangosaurus</i>	0 0 0 0 0	0 0 0 0 1	0 0 0 0 0	0 0 0 0 ?	? 0 ? 0 0	0 0 0 ? ?	1 0 0 0 0	0 0 1 0 0	0	87.8

Note: Characters are listed numerically to correspond with those presented in the text. Primitive states scored with a “0”, missing data with a “?”, and all others indicate the derived condition. The symbol “%” refers to the percentage of character states scored for each taxon.